SUPPORTING INFORMATION

Twisted Light-Enhanced Photovoltaic Effect

Kristan Bryan Simbulan[1,2], Yi-Jie Feng[1], Wen-Hao Chang[3], Chun-I Lu[1], Ting-Hua Lu[1], and Yann-Wen Lan[1]**

[1]Department of Physics, National Taiwan Normal University, Taipei 11677, Taiwan
[2]Department of Mathematics and Physics, University of Santo Tomas, Manila 1008, Philippines
[3]Department of Physics, National Taiwan University, Taipei 10617, Taiwan

* *Corresponding Authors*

Atomic force microscopy measurement on the monolayer MoS_2 channel

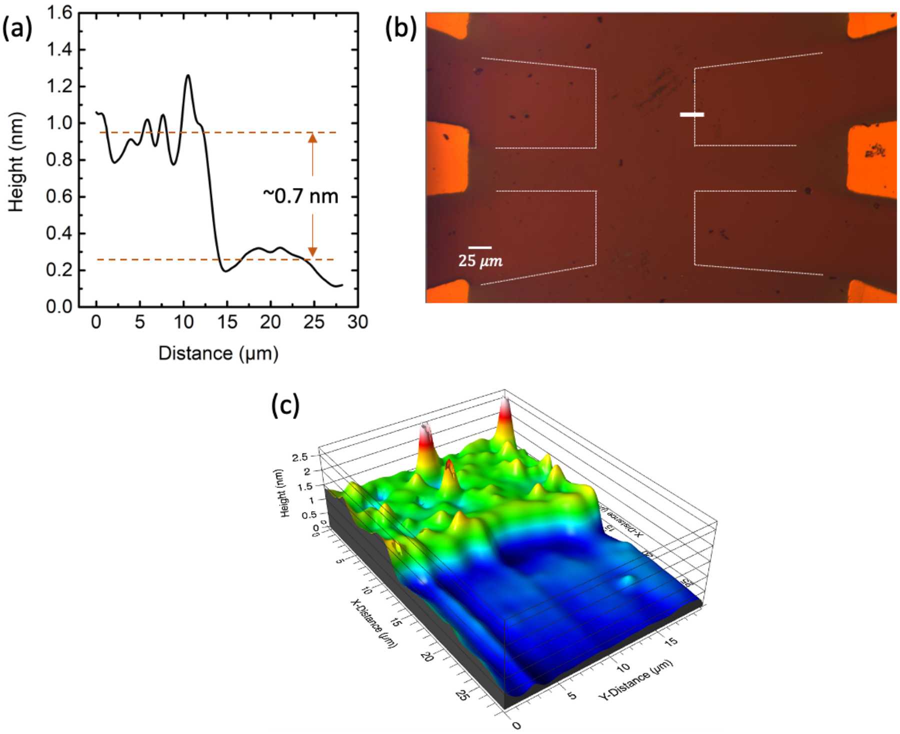

Figure S1. Atomic Force Microscopy measurement on the monolayer MoS_2 channel. (a) The height profile of the region crossing the border between the MoS_2 film and the SiO_2 substrate as indicated by a white bar in **(b)**. The white bar has a length of ~25 µm. **(c)** The 3D image of the AFM profile in the vicinity of the same sample portion indicated in (b) [3D image processed using ProfilmOnline, KLA Corporation, 2021].

Optical setup: Laguerre Gaussian beam generation

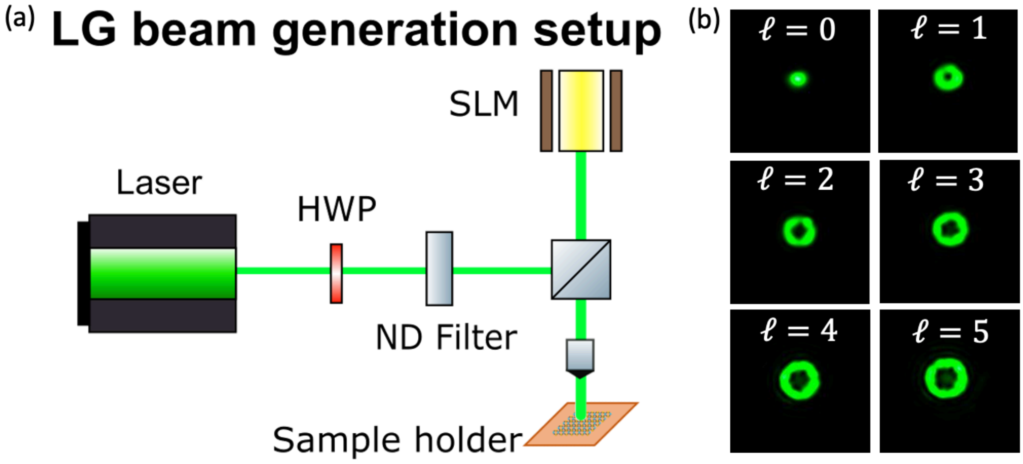

Figure S2. Laguerre-Gaussian beam generation setup. **(a)** The general optical setup for the generation of Laguerre Gaussian (LG) beam. The critical component in converting a Gaussian beam to LG light is the Spatial Light Modulator (SLM), which modulates the phase of the incident beam using computer holograms. HWP and ND Filter refers to the half-wave plate and the neutral density filter, respectively. **(b)** The resulting LG beam spots are presented according to selected values of ℓ with a constant radial index equal to zero.

Electrical measurements on the monolayer MoS_2 while illuminated with light of different OAM conditions

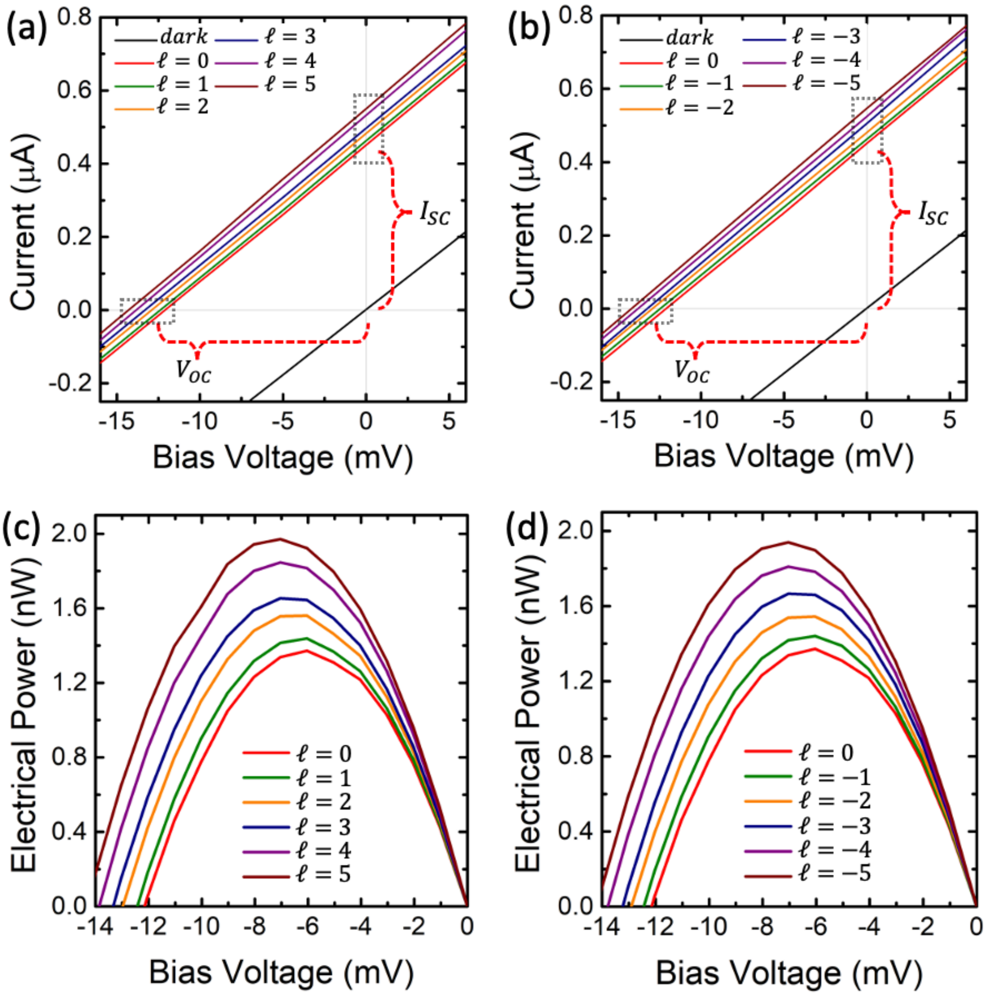

Figure S3. IV Characteristics. The IV characteristic curves measured while the device channel is illuminated by light with **(a)** positive and **(b)** negative values of ℓ. The electrical power *versus* bias voltage chart for **(c)** positive and **(d)** negative ℓ conditions.

Another set of electrical measurements on the monolayer MoS_2 channel device at fixed 100 μW laser power

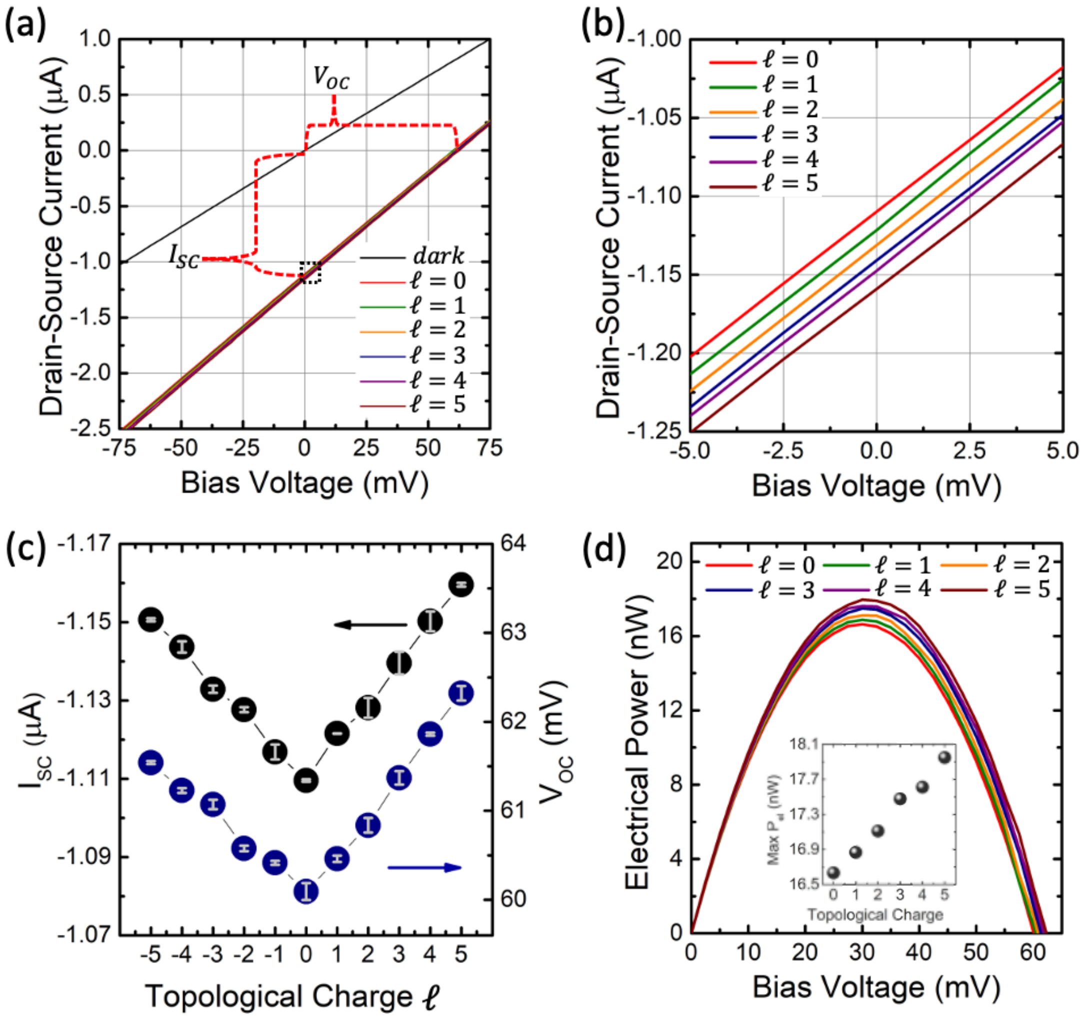

Figure S4. Enhancement of the photovoltaic effect in monolayer MoS_2. (a) Drain-source current *versus* bias voltage characteristic of the device in the dark and under illumination of light with different ℓ (4× objective lens, 100 μW laser power, 532 nm wavelength). **(b)** Zoomed-in portion of the region enclosed by the dotted black square in (a). **(c)** The corresponding I_{SC} and V_{OC} at various ℓ, and the **(d)** generated electrical power *versus* bias voltage of the device extracted from (a).

A set of electrical measurements on the second monolayer MoS_2 channel device at fixed 100 μW optical power

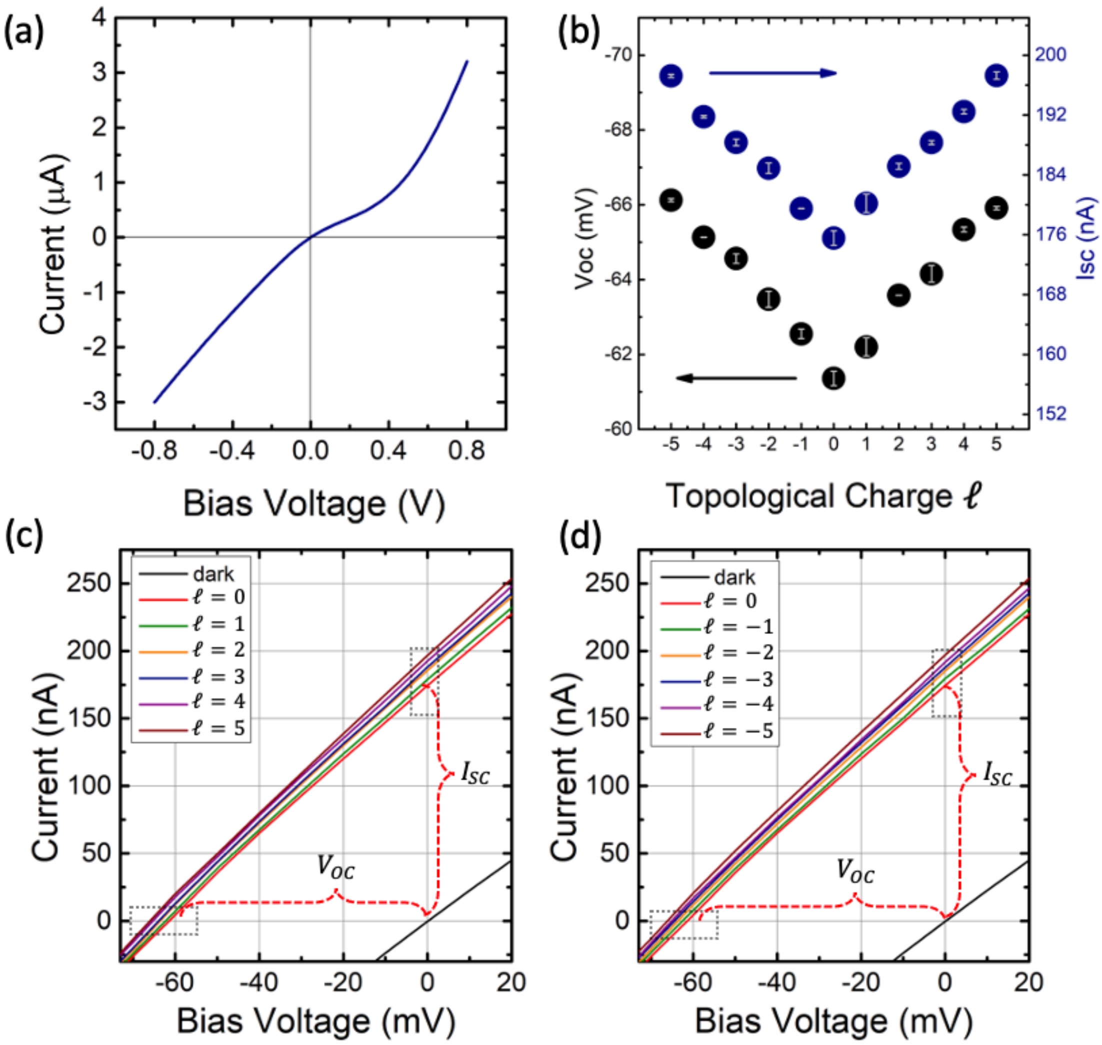

Figure S5. IV curve measurements on another device of similar structure as the one in the manuscript. (a) The IV curve of the device under dark condition. This second device apparently have higher channel resistance, manifested by a lower device current, compared to the device featured in the manuscript. This may be due to the presence of more defects in the device, giving it a more "diode-like" behavior. **(b)** The recorded I_{SC} and V_{OC} from this device at different light conditions. The overall increase in I_{SC} is relatively lower in this device more likely due to the presence of more defects. The error bars were derived from three measurements for each light condition. The representative IV curves measured while the device is illuminated with **(c)** positive and **(d)** negative ℓ conditions (4× objective lens, 100 μW laser power, 532 nm wavelength).

PL Measurements on the monolayer MoS_2 using incident light of various OAM

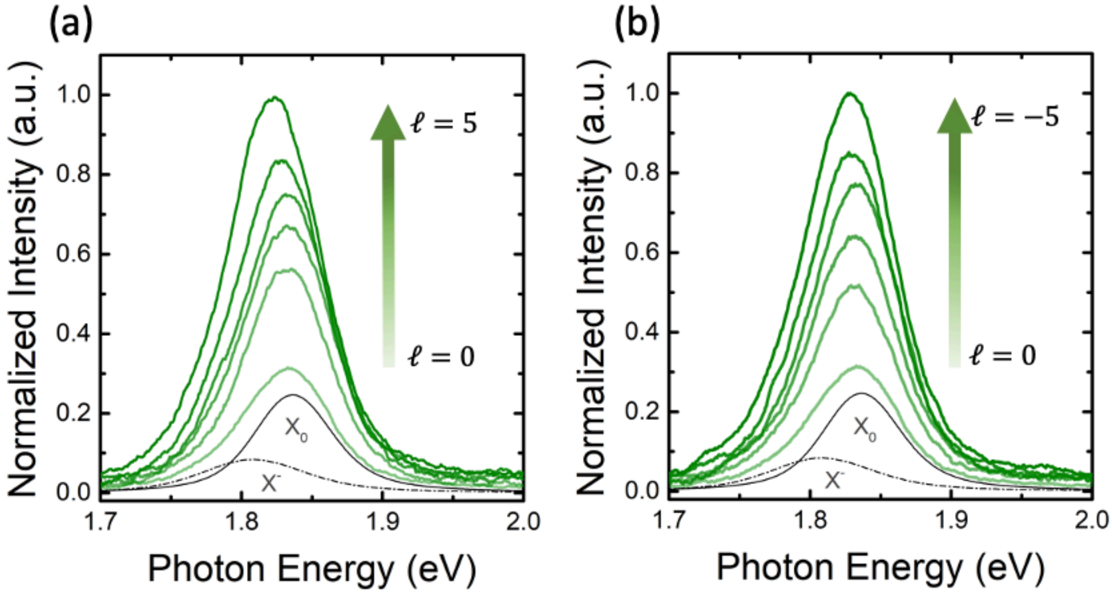

Figure S6. Photoluminescence spectra. The Photoluminescence spectra measured simultaneously with the IT curve in Fig. 3(a) for **(a)** positive ℓ and **(b)** negative ℓ conditions (all including $\ell = 0$ or the fundamental mode). Only the fitted exciton and trion peaks for $\ell = 0$ is shown in both (a) and (b) to tidy up the graphs.

Detailed peak fittings of the measured PL spectra

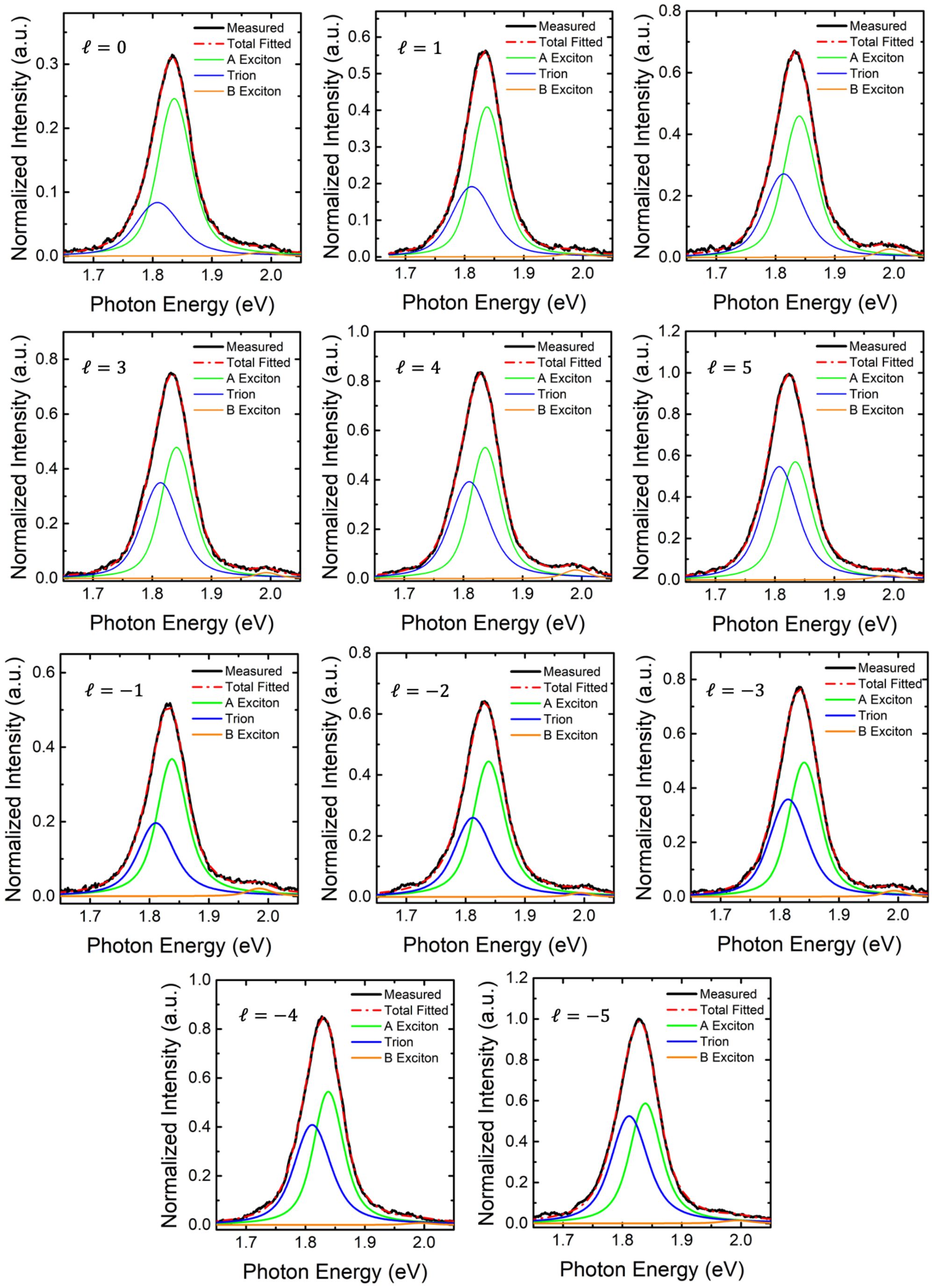

Figure S7. Peak-fitted PL curves. Curve fitting results of the PL spectra in Fig. 3(b) in the main manuscript.

Estimating the absorption efficiency

To estimate the absorption efficiency, η, we used the equation,

$$V_{OC} = \frac{kT}{q} \ln\left(\frac{(N_D + \Delta n + p_t)(\Delta p)}{n_i^2}\right), \qquad [1]$$

that considers the intrinsic (n_i), doping (N_D), and photogenerated ($\Delta n = \Delta p$) carriers, as well as the reported effective photoconductive gain in the form of trapped hole concentrations p_t. The estimated values of n_i and N_D are (~10^{10} cm^{-2}) [1, 2] and (~10^{12} cm^{-2}) [3], respectively. The formula for finding Δn is $\Delta n = \phi\tau_r = \frac{\eta P_{laser}\lambda}{A_{ph}hc}\tau_r$, where η is the absorption efficiency, λ the wavelength of the incident light (532 nm), A_{ph} the illuminated area, h Planck's constant, c the speed of light, τ_r the carrier recombination lifetime (~100 ps) [4], and $\phi = (\eta P_{laser}\lambda)/(A_{ph}hc)$ the photon flux. The density of trapped hole states can be expressed as $p_t = (\phi P_t \tau_r)/\left(\phi\tau_r + P_t\frac{\tau_t}{\tau_g}\right)$, where P_t is the total density of hole trap states (~10^{10} cm^{-2}), and τ_t and τ_g the hole trapping and release time, respectively, in which ratio $\frac{\tau_g}{\tau_t}$ is fixed and was assumed to be ~ 200 as adapted from a previous study [4]. Using all the given values, **Eq. 1** is fitted with measured V_{OC} at different values of the ℓ of the incident light to get the estimated absorption efficiency, η.

References:

[1] Hong, J.; Hu, Z.; Probert, M.; Li, K.; Lv, D.; Yang, X.; Gu, L.; Mao, N.; Feng, Q.; Xie, L.; Zhang, J.; Wu, D.; Zhang, Z.; Jin, C.; Ji, W.; Zhang, X.; Yuan, J.; Zhang, Z. Exploring Atomic Defects in Molybdenum Disulphide Monolayers. *Nat. Commun.* **2015**, *6* (1), 6293.

[2] Chae, W. H.; Cain, J. D.; Hanson, E. D.; Murthy, A. A.; Dravid, V. P. Substrate-Induced Strain and Charge Doping in CVD-Grown Monolayer MoS_2. *Appl. Phys. Lett.* **2017**, *111* (14), 143106.

[3] Wu, C.-C.; Jariwala, D.; Sangwan, V. K.; Marks, T. J.; Hersam, M. C.; Lauhon, L. J. Elucidating the Photoresponse of Ultrathin MoS_2 Field-Effect Transistors by Scanning Photocurrent Microscopy. *J. Phys. Chem. Lett.* **2013**, *4* (15), 2508–2513.

[4] Furchi, M. M.; Polyushkin, D. K.; Pospischil, A.; Mueller, T. Mechanisms of Photoconductivity in Atomically Thin MoS_2. *Nano Lett.* **2014**, *14* (11), 6165–6170.